Modeling of Selected SFF Process Limits

Patricio Mendez, Stuart Brown

Department of Materials Science and Engineering
Massachusetts Institute of Technology

Abstract

An analytical model of the thermal field for one scan line during SLS is developed. Quantitative relationships between net heat input and beam velocity are stated for sintering at a given distance from the center of the beam and for the case of maximum surface temperature. For the maximum surface temperature, two extreme cases have been analyzed: pure conduction heat transport, and highly convective molten consolidation. It is suggested that a highly convective process allows significantly higher net heat input than pure conduction. It is found that for certain conditions, the relationship between net heat input and beam velocity is independent of the thermal conductivity of the material. Key Words: model, melting, selective laser sintering, thermal, process window.

Introduction

For a reaching a desired sintering depth, the velocity of the laser beam over the surface of the powder layer during SLS depends on the net heat input. It is generally necessary to impose a higher heat input to increase beam velocity while maintaining the same sintering depth. The temperature reached at the surface limits the heat flux. This work focuses on these thermal aspects.

The sintering process is characterized by a sintering temperature (T_s) and sintering time (t_s). These parameters are such that for reaching a desired void fraction or smaller, the powders have to remain at a temperature of at least T_s during at least t_s, and can be estimated with an appropriate sintering model (for example ref. 1 or 2). In the case of melting powders, the sintering time can be considered small and the sintering temperature corresponds to the melting temperature, or the temperature of the peak specific heat in the case of a melting range. In both cases, sintering or melting, the temperature field after the beam passes can be approximated by a thin layer of hot material at the surface.

The mechanism governing consolidation process dictates the maximum surface temperature. For some materials and process conditions, for example polymers or wax, complete melting of the powders occurs under the beam (ref. 3). In other cases a solid phase is always present, for example polymer coated silicon carbide (ref. 2). In the latter case, the physics of the process can be studied as a heat conduction problem, neglecting the presence of some melting. When all the powder is molten, and convective currents help to homogenize the temperature within the liquid, the problem requires a detailed analysis of the effect of flow and the heat conduction with a moving boundary. In this work, the two cases are analyzed. For the melting controlled problem a limiting case is taken, where convective currents completely homogenize the temperature of the liquid, and the deepening velocity of the melting front (V_m in fig. 4) is high.

Modeling the entire SLS process is very difficult due to the many different physical processes involved. For the case of fully molten powder, surface forces change the shape of the sintered line, making it narrower and

convex. This work does not consider these effects and those due to shrinkage and distortion. The geometry of the process will be assumed to be a flat surface throughout the following analysis.

The net heat input is related to the laser power through an optical coupling coefficient (ref. 4). The thermal conductivity of the powders is estimated from that of solid material using the semi-empirical model proposed by Xue and Barlow (ref. 5). For the typical conditions in SLS, the heat transfer problem can be considered one dimensional. (ref. 7). For simplicity of the analytical solutions, the laser beam will be considered as a round uniform surface flux that moves in the direction of x in the moving coordinate frame of Fig. 1. The fact that the heat source can be better described by a gaussian distribution, or that there may be some volume heating in a semi transparent absorbent medium (ref. 4) does not affect the final calculation of the depth, since the temperature field after the beam passed can be approximated by a thin hot surface layer, independent of how the stored energy was added. The surface of the powder layer, with the exception of the zone under the beam will be considered insulated without surface heat losses due to convection or radiation.

Variables not defined within this paper follow the standard definition associated with heat transfer analysis.

Conduction Model

This model considers conduction as the only mechanism of heat transfer. It is assumed that the thermal properties of the body are constant and the heat of melting is negligible. This means that the sintering zone and the powder are considered to have the same thermal properties regardless of temperature.

The one dimensional analytical solution for a moving heat source, like that of Fig. 1, is given by eq. (1) to (4).

$$T(z,t) = \frac{q}{k} 2\sqrt{\alpha t}\,\mathrm{ierfc}\left(\frac{z}{2\sqrt{\alpha t}}\right) \qquad \text{for } t \le \tau \qquad (1)$$

$$T(z,t) = \frac{q}{k} 2\sqrt{\alpha t}\,\mathrm{ierfc}\left(\frac{z}{2\sqrt{\alpha t}}\right) - \frac{q}{k} 2\sqrt{\alpha (t-\tau)}\,\mathrm{ierfc}\left(\frac{z}{2\sqrt{\alpha (t-\tau)}}\right) \qquad \text{for } t > \tau \qquad (2)$$

$$t = \frac{\sqrt{r^2 - y^2} - x}{V} \qquad (3)$$

$$\tau = 2\frac{\sqrt{r^2 - y^2}}{V} \qquad (4)$$

The temperature profile at the sintering depth and width ($z = d, y = w$), and the isotherm for the sintering temperature at the plane of symmetry ($y = 0$) are shown in Fig. 2 and 3. It can be seen in Fig. 3 that the characteristic length for heat diffusion in the depth direction is much smaller than in the surface direction (axis x and z have different scales).

Eq. (1) gives the temperature field for points under the beam. Eq. (2) represents the diffusion of heat into the bulk of the powder, after the beam has passed. Eq. (3) and (4) connect the one dimensional model and the moving source geometry.

Those points where $T = T_s$ during a time t_s provide the shape of the sintered section in the y = constant plane. For each of these planes we have to find the roots of $T(z,t) = T_s$, and find the depth (z), for which

the difference between the roots is the sintering time t_s. Eq. (2) has no explicit expression for the roots of $T(z, t) = T_s$, so we simplify its form. The first step of this simplification is to consider the process of diffusion of heat into the bulk as diffusion of heat from a thin layer of hot material at the surface. The second step is to approximate the isotherms $T = T_s$ with ellipses.

Eq. (5) corresponds to the thin film simplification. For the representative case analyzed, this approximation is very accurate, as can be seen in Fig. 2 and 3.

$$T(z, t) = \frac{\alpha q \tau \exp\left(\frac{-z^2}{4\alpha t}\right)}{k\sqrt{\pi \alpha t}} \tag{5}$$

Here $t = -x/V$. The corresponding equation for an ellipse approximating the isotherms corresponding to a plane y = constant is:

$$\left(\frac{x+a}{a}\right)^2 + \left(\frac{z}{b}\right)^2 = 1 \tag{6}$$

This ellipse must have the same depth and the same length as the sintering isotherm. The length $2a$ is obtained from eq. (5) solving for x with $T = T_s$ and $z = 0$. This length varies with the y coordinate.

$$a = \frac{\alpha V}{2\pi}\left(\frac{q\tau}{kt_s}\right)^2 \tag{7}$$

The depth of the ellipse (b) is obtained by maximizing eq. (5) with respect to t to find T_{max}, and solving eq. (5) for z with $T = T_s$ and $t = t_{max}$.

$$b = \sqrt{\frac{2}{\pi}} e^{-1/2} \frac{\alpha q \tau}{k T_s} \tag{8}$$

The ellipse corresponding to the representative case analyzed is plotted in Fig. 3. It can be seen that the position of the maximum is shifted, but the distance corresponding to the sintering time remains approximately the same. Taking the desired sintering depth, sintering time, and scan width as d, t_s and $2w$ respectively, in eq. (6) $z = d$, $x + a = Vt_s/2$, and in eq. (4) $y = w$.

For the representative case analyzed, the term containing x in eq. (6) is small up to sintering times of 0.45 s. In the following example we consider the melting of nylon powders, therefore, sintering time is negligible and this term will not be considered. Substituting eq. (7) to (8) in (6), and using the identity $q = Q/\pi r^2$, we obtain the relationship between Q and V for a certain sintering material and geometry:

$$Q = \left(\frac{\pi}{2}\right)^{3/2} e^{1/2} \frac{\rho c T_s r d}{\sqrt{1 - \left(\frac{w}{r}\right)^2}} V \tag{9}$$

Eq. (9) gives the minimum net heat input necessary for sintering a certain depth at a certain speed.

Maximum Surface Temperature Assuming Conduction

There is also a maximum heat input, given by the maximum surface temperature that can be reached before

undesired effects occur (laser ablation (ref. 6), pyrolysis (ref. 3), boiling). For the cases in which conduction is the only heat transfer process (e.g. when there is no melting), the maximum surface temperature is obtained from eq. (1), for $z = 0$, $y = 0$ and $t = \tau$:

$$T_{max} = \frac{1}{\sqrt{\pi}} \frac{q}{k} 2\sqrt{\alpha t} \tag{10}$$

Rearranging eq. (10), we obtain the relationship between net heat input and velocity for a given maximum surface temperature $T_{max} = T_c$.

$$Q = \left(\frac{\pi}{2}\right)^{3/2} \frac{k r^{3/2} T_c}{\sqrt{\alpha}} \sqrt{V} \tag{11}$$

Melting controlled model

When there is complete melting of the powders between the surface and the sintering depth, convective currents can occur, and a pure conduction model is not appropriate. In these cases the sintering temperature corresponds to the melting point.

We analyze the limiting case in which convection current homogenize the liquid temperature (Biot << 1), and the velocity of deepening of the melting front is sufficiently high (Peclet >> 1) to consider that there is no heat lost by conduction (Fig. 4).

This model represents the heating of points under the beam and provides an estimate of maximum surface temperature. Once the beam has passed, the thermal field can be analyzed with eq. (5) as heat diffusing from a thin hot surface layer.

An energy balance for this case is:

$$q\tau = \rho\beta \left[c_{p_p} T_m + \Delta H_m + c_{p_l} (T_l - T_m) \right] + Q_{cond} \tag{12}$$

where we neglect Q_{cond} for high values of the Peclet number.

An energy balance of the heat transfer at the melting front gives:

$$\rho\beta \left(c_{p_p} T_m + \Delta H_m \right) + Q_{cond} = Q_{conv} \tag{13}$$

where

$$Q_{conv} = \int_0^{\tau} h_t (T_l - T_m)\, dt = h (T_l - T_m)\, \tau \tag{14}$$

Combining eq. (12) and (13), and neglecting Q_{cond}, we obtain the heat input corresponding to a given homogeneous liquid temperature (T_l).

$$Q = \pi r^2 h (T_l - T_m) \frac{c_p T_l + \Delta H_m}{c_p T_m + \Delta H_m} \tag{15}$$

In eq. (15) the heat capacity of liquid (c_{p_l}) and the solid (c_{p_s}) are assumed to be the same.

The Peclet and Biot numbers are estimated using the depth reached at the end of the beam β as the characteristic length, where $\beta = q\tau/\rho\,(c_p T_l + \Delta H_m)$.

Representative Case

The representative case considered is the SLS of Laserite nylon with a velocity of 12.7 mm/s, a sintering depth of 0.317 mm, and a scan spacing of 0.5 mm.

The value of the parameters used are presented in Table 1.

Table 1: Parameters for the Representative Case

Process	Solid Material	Powder
V = 12.7E-3 m/s	T_m =188.7 °C	$\varepsilon = 0.4$
r = 1.5E-3 m	T_c = 1000 °C	$\rho = 624$ kg/m^3
d = 0.317E-3 m	$T_s = T_m$	k = 0.1 W/m-K
w = 0.25E-3 m	c_p = 1968 J/kg-K	α = 8.14E-8 m^2/s
T_{amb} = 25 °C	ΔH_m = 55688 J/kg	
	ρ_s = 1040 kg/m^3	
	k_s = 0.23 W/m-K	

From eq. (11) we obtain the necessary heat input for sintering: Q = 4 W. Eq. (10) gives the maximum surface temperature T_{max} = 910.6 °C, The dimensions of the ellipse corresponding to the sintering width are $a \approx 11$ mm and $b \approx 0.3$ mm.

The hypothesis of one dimensional heat transfer is valid for all depths (within a 5% error) when $V^2\tau/4\alpha$ > 4.4 (ref. 7). For the representative case, this is equivalent to $|y/r| < 0.9993$, i.e., almost all points under the beam approximate 1D heat transfer.

An energy balance indicates that the heat losses by convection and radiation are negligible. During the time it takes to reach the maximum depth at the plane of symmetry (t_{max}), the energy input is $q\tau$ = 134 kJ/m^2. After the beam has passed, the losses by convection account for 0.7%, by radiation 2%; the heat flux by conduction through the sintering isotherm accounts for 32%, and the energy stored between the surface and the sintering isotherm is 68%. In this analysis the heat of melting was neglected; included, it accounts for 12% of the energy stored. An approximate consideration of the heat of melting can be made by increasing the specific heat of the powder by 12%. During the time the beam is over a point, the radiation losses are 7% of the net energy input. This amount must be considered in the overall efficiency of the laser beam.

From eq. (8) it can be inferred that the maximum temperature decreases with increasing depth. A medium is considered semi-infinite when it is deeper than the penetration corresponding to a small temperature increase. For $T = 0.05 \times T_s$, we obtain a depth of $20b$ for the plane of symmetry. In this example, the minimum depth is 6.4 mm (approx. 20 layers).

For the melting controlled model we use representative values for the convection coefficient and for the thermal conductivity of the liquid corrected for convective flow. A typical value for the convection coeffi-

cient in liquids is $h = 1000$ W/m^2-K. A more accurate estimation of h requires a detailed study of the convective flow and liquid properties. The thermal conductivity of the liquid will be estimated as ten times the conductivity of the solid material ($k_l = 2.3$ W/m-K). From eq. (15), for a net heat input $Q = 4$ W, the corresponding liquid temperature is $T_l = 436$ °C. This temperature rise is approximately half of that for the pure conduction model. For a maximum temperature of 1000 °C, the maximum net heat input is 30 W.

The values of β and Pe are 0.25 mm, and 3.2 respectively. The Peclet number is greater than 10 for velocities lower than 4 mm/s. The value of Bi is 0.1, indicating that heat conduction and convective currents act to homogenize the liquid temperature.

Discussion and Conclusions

The analysis described in this article is meant both to provide some physical insight into the SLS process and to guide directions for further analyses including thermal and mechanical effects. Note that many process parameters, such as energy flux, scan rate, and beam radius, enter into the presented relations linearly. In some cases this linearity results from our simplifications in analysis. The actual process obviously contains more nonlinearities and complexities than we represent here. However, we believe that these relatively simple relations represent the first order physics of the process and therefore provide functional guidance on the effect of different process variables.

The relations we derive can also be used to estimate scan rate and heat flux windows for feasible SLS processing. Fig. 5 presents one such process window for Laserite nylon. Note that the thin film solution of heat transfer into the bulk after the beam has passed a given point is common to both the conduction and melting controlled models. The models differ, however, in calculating the temperature field immediately under the beam. The three curves in the figure illustrate the thin film solution and consequences of this difference in temperature field. The lower straight line represents the thin film solution and is a boundary of the process window. The intersecting curve represents the other boundary from the conduction model which is formed by assuming a limiting maximum surface temperature. Together the two boundaries define a process window assuming conduction control of the process. Combining eq. (9) and (11), we obtain the theoretical maximum velocity and heat input that allow sintering to the desired depth and width, without reaching the critical surface temperature.

$$V_{max} = e^{-1}\alpha r\left(\frac{T_c}{T_{sd}}\right)^2\left(1-\left(\frac{w}{r}\right)^2\right) \tag{16}$$

Using the parameters of the representative case, eq. (16) gives $V_{max} = 15$ mm/s. Values of scan rate and incident energy (assuming an optical coupling of 50 percent) taken from a video study provided by the SLS research group at the University of Texas as Austin (ref. 3) are plotted as points in the figure. The video image corresponding to the left point pictured the formation of vapor bubbles. We used the process parameters corresponding to the right point as our representative case for analysis.

The upper line in the figure represents the process boundary assuming melting control, where the molten material is isothermal. It can be seen that the working window in this case is potentially larger, due to a more homogeneous distribution of the thermal energy under the beam. In this case, the molten zone is able to store more energy before reaching the critical temperature. Confirmation of this effect would require a more accurate estimation of the parameters for the convection in the liquid. In the example typical values have been used.

In a sintering process without melting, the model pure conduction model applies. However, when there is melting involved, the process may not be melt controlled. A detailed study of the flow currents is necessary, and depending on its characteristics, the ruling mechanism is melting, pure conduction (for the case in which there are almost no currents), or mixed.

In this model the value of the thermal properties of the body are considered constant, therefore the Fourier equation of heat conduction is linear and it is possible to superimpose solutions. Due to the simplicity of the model, this can be accomplished efficiently and with a moderate computer overhead making it possible to consider the effect of different passes over the same point to calculate a total temperature history. A study addressing the effect of multiple passes could explain the effect of the beam radius on the sintering depth. For the case of multiple passes, increasing the beam diameter increases the depth of sintering (ref. 8). For the case of a single pass, eq. (9) indicates the opposite effect.

Acknowledgments

This work was funded primarily by the Office of Naval Research (grant number N00014-94-1-0181). We would like to acknowledge substantial assistance provided by the research effort in SLS at the University of Texas at Austin, and also the important suggestions and comments of the other students in Professor Brown's research group, G. Trapaga and V. Meli.

References

1. Sun, M., Nelson, J. C., Beaman, J., Barlow, J. 1991 (August). *A Model for Partial Viscous Sintering*. Solid Freeform Fabrication Symposium, Proceedings. University of Texas at Austin, pp. 46-55.

2. Nelson, J. C., Vail, N. K., Barlow, J. W. 1993 (August). *Laser Sintering Model for Composite Materials*. Solid Freeform Fabrication Symposium, Proceedings. University of Texas at Austin, pp. 360-369.

3. Das, S., Pogor, B. *Video Microscopy Experiments on SLS of Polycarbonate, Wax and Nylon*. Unpublished, The University of Texas at Austin, April 25, 1994.

4. Sun, M., Beaman, J. 1991 (August). *A Three Dimensional Model for Selective Laser Sintering*. Solid Freeform Fabrication Symposium, Proceedings. University of Texas at Austin, pp. 102-109.

5. Xue, S., Barlow, J. 1991 (August). *Models for The Prediction of the Thermal Conductivities of Powders*. Solid Freeform Fabrication Symposium, Proceedings. University of Texas at Austin, pp. 62-69.

6. Deng, X., Zong, G., Beaman, J. J. 1992 (August). *Parametric Analysis for Selective Laser Sintering of a Sample Polymer System*. Solid Freeform Fabrication Symposium, Proceedings. University of Texas at Austin, pp 102-109.

7. Festa, R., Manca, O., Naso, V. *A Comparison Between Models of Thermal Fields in Laser and Electron Beam Surface Processing*. Int. J. Heat Mass Transfer. Vol. 31, No. 1, pp. 99-106, 1988.

8. Nelson, J. C. *Selective Laser Sintering: A Definition of the Process and an Empirical Sintering Model*, Ph.D. dissertation, The University of Texas at Austin, 1993.

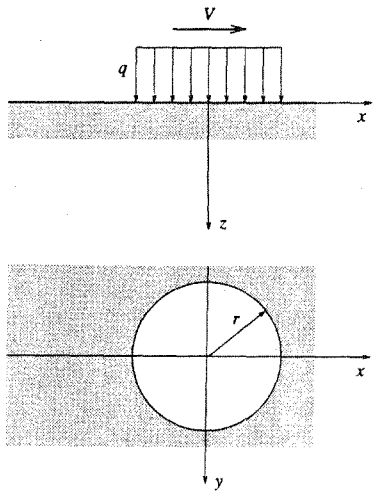

Figure 1

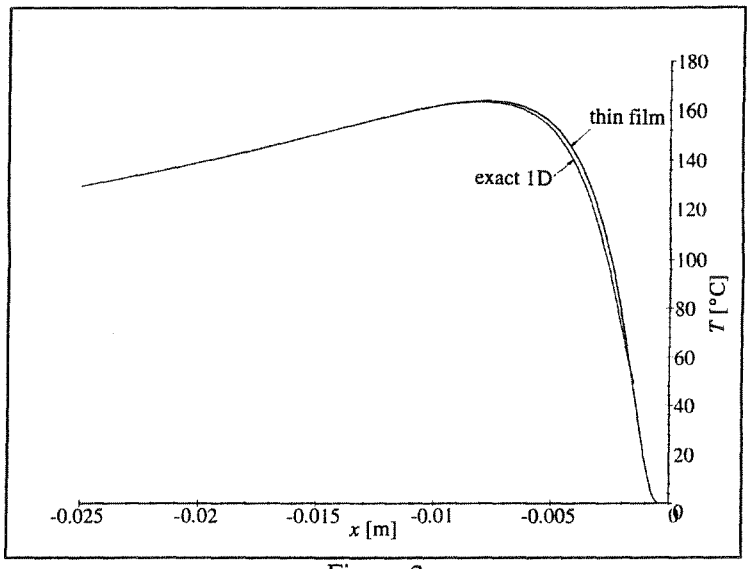

Figure 2

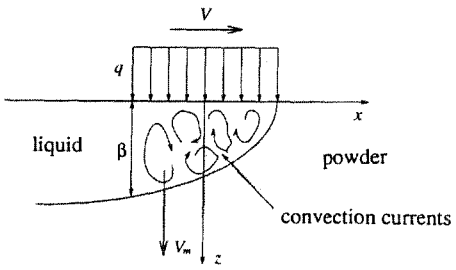

Figure 4

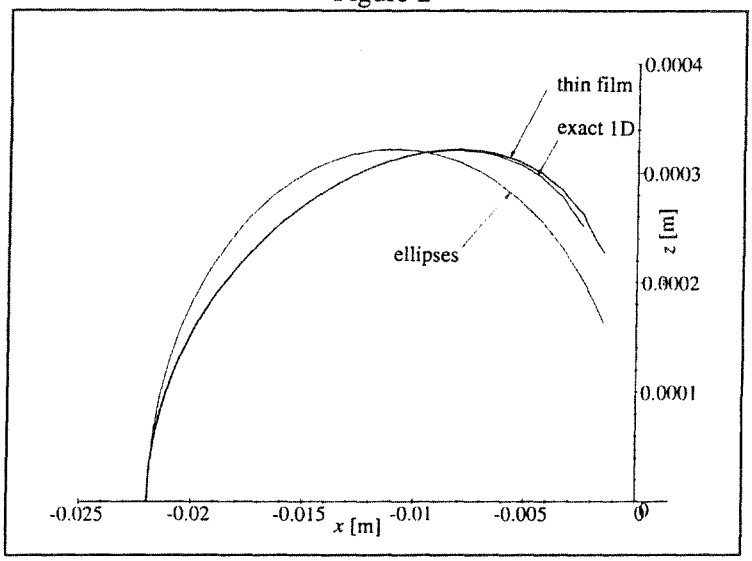

Figure 3

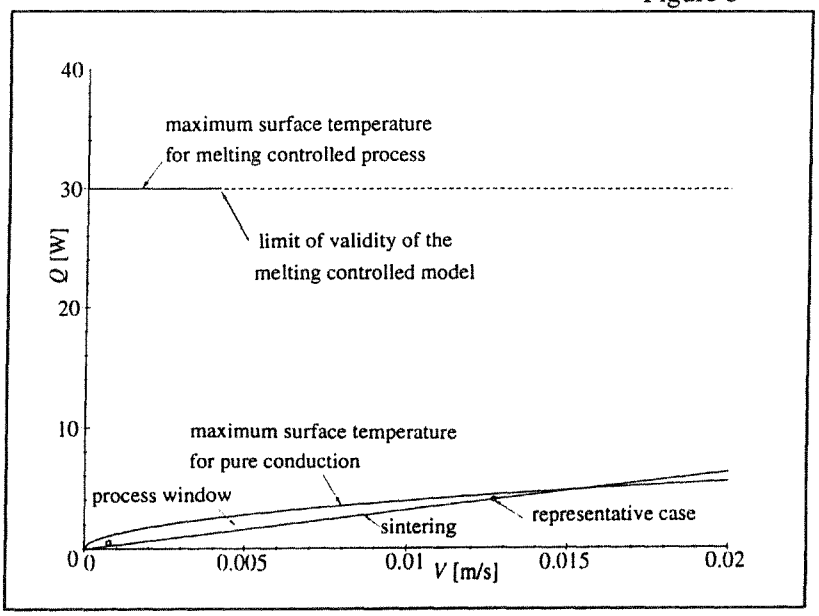

Figure 5

APPLICATIONS OF
3D LASER DIGITIZING AND SURFACING TECHNOLOGIES

Many companies have manufacturing requirements to copy or "reverse engineer" an already existing part for which there is no existing CAD model, print, pattern, or mold. In the past this process has been very tedious requiring weeks and sometimes months to complete. The engineer has to create a CAD model by measuring the physical part with calipers and/or a CMM and then create features and surfaces in CAD. If a 2D print is available, this data must be converted to define the CAD model features. This process is very prone to error and several iterations must be executed before an acceptable completed part is produced.

There is now an available process to support "reverse engineering" applications which greatly reduces the time to complete these projects, provides a complete and accurate CAD model on the first iteration, allows for the programming of tool paths, and is completely compatible with the company's current CAD/CAM procedures. This process includes the integration of the automated 4-axis 3D laser digitizing from Digibotics, Inc. with a complete software environment for point processing, surface generation, and analysis from Imageware. A case study using these technologies was recently completed by Fred Nicholas, CAD/CAM Manager, of InterMotive Technologies, a design and engineering company located in Belleville, MI. This paper describes the entire flow through the digitizing, surfacing, and CAD/CAM processes.

For this case study, Mr. Nicholas selected an automotive thermostat housing which is a part with some complex outer surfaces and an internal cavity. A core stick of the internal cavity was created. The Digibot II 3D laser digitizer from Digibotics, Inc. was used to digitize both the external part and the internal core stick. After editing the 3D digitized data, a point file was imported into the Surfacer software system from Imageware. Surfacer was used to create a network of B-spline curves and surfaces. An IGES NURBS surface file was created and then imported into several CAD/CAM systems to demonstrate the ability to create a surface and tools paths for making the part. For this case study, the Computervision CADDS5 software was used to demonstrate the complete CAD/CAM process.

The Digibotics 3D laser digitizing technology was used for this project because it offers several unique advantages for "reverse engineering" of complex parts. The Digibot II is an automated 4-axis digitizer that provides a simple, accurate, and quick way to copy or inspect complex sculpted surfaces. After fixturing an object, the user specifies a point density and instructs the system to begin. While digitizing, the object

rotates on the platter and the laser translates horizontally and vertically. Vertically spaced cross-sections are digitized starting from the bottom and moving upward. The Digibot Adaptive Scanning Software intelligently follows the contours of the surface acquiring a sequence of adaptively spaced points while keeping the laser beam normal to the surface. Concave surfaces and multiple contours are obtained by pivoting the laser about obstructing surfaces. After digitizing, the object is composed of a stack of cross-sectional contours. The entire object along with individual points and contours can be examined and modified as needed using the Digibot Data Editor. A surface mesh composed of triangular facets is generated by connecting points and contours between cross-sections. The resulting polyline and/or surface mesh can be exported via data formats such as DXF, STL, VDA, or IGES.

The Surfacer software system provides the link between the 3D laser digitized data and the conventional CAD/CAM system. Surfacer accepts point data directly from the Digibot Editor and performs point data analysis and processing such as segmentation, sectioning, filtering, and feature extraction. The NURBS surfaces are then quickly and accurately created from the selected point sections. The quality of the created surfaces are verified by points to surface comparison, reflectance analysis, curvature analysis, and cross-sectional tools. These surfaces can then be edited and/or modified. Point, curve and/or surface geometry can then be exported directly to "downstream" processes such as CAD, CAM, Analysis or Visualization/Animation systems.

The first step of the process was to digitize the thermostat housing using the Digibot II 3D laser digitizer. The housing was attached to the platter of the Digibot II by simply using hot glue. The Digibot II then digitized the entire housing by using Digibotics' patented adaptive scanning procedure. Both the external housing and the internal core stick were digitized. In a post-processing phase, Mr. Nicholas viewed the 120 cross-sections and performed minor editing to guarantee a good clean file of 3D data points. The digitizing and editing process for this housing was completed in 1 1/2 days. Mr. Nicholas also used the Digibotics Triangulator and STL Generation software to create an STL file of the housing. The Accelerated Technologies Inc. DTM rapid prototyping system was used to create a polycarbonate copy of the housing. This is very useful as an intermediate step to demonstrate that the digitizing process was very complete and accurate.

The two files of 3D data points (containing about 20,000 points) were then imported directly into Surfacer for creation of the surfaces. The two data files were first combined to form one complete external and internal object by registering the two

parts to a common axis through the centroid of the part. Surfacer provides a complete set of tools for aligning multiple scans or aligning scan data to CAD data. A "push-button" surface of the entire housing was then created. This one large complex NURBS surface is very useful for visualization, for gross product testing, and for interference checking with other CAD components. Because the Digibot digitized data is created in orderly well-spaced cross sections with no redundant or over-lapping data, this makes it much easier for Surfacer to create surfaces and perform its analysis functions. After the point analysis and registration, individual accurate surfaces were created. This occurs by generating surface patches over different point sections to define unique surfaces. Surfacer provides tools for detecting surface edges and segmenting points to define areas to be surfaced. Surface patches can then be fit to the points, with the user having control over the NURBS smoothness and fitting tolerances. For the housing, 21 different surface patches were created. These patches are stitched to create continuous, "watertight" connections, and different analysis was performed to confirm the accuracy of the surfaces. The 21 surface patches were then converted to an IGES 5.0 NURBS surface file for export into the CAD/CAM systems. This processing time in Surfacer took about two working days.

Mr. Nicholas then imported the IGES file into CADDS5 for processing. The file was also imported into ProEngineer and AutoCAD to demonstrate the IGES compatibility with other CAD systems. In CADDS5, a complete solid model was created by sewing the 21 individual surfaces. With this solid model, physical property analysis can then be performed such as volume and mass calculations. An STL file was created from this solid model, and a prototype was created using the 3D Systems rapid prototyping system. A tool path was created using Computervision's CVNC software. The internal cavity was first isolated from the external part for tool path generation. Then a tool path was generated on the external surface. Finally, a product drawing was generated for documentation of this part. The detailing environment included all radii, dimensions, cutting sections, tolerances, and information for placing the housing in its engine position. The procedures implemented in CADDS5 are very straight forward and utilizes the normal CAD/CAM functions that would be used for any solid model design. The procedures for CADDS5 were executed in two working days.

The processes that are demonstrated in this case study were not available one year ago. There has been tremendous progress during this time in the integration of the digitizing hardware/software and surfacing software for supporting these complex projects. This case study was implemented in about one week, and is at least a four week improvement over uses of other approaches. The Digibotics and Imageware

week improvement over uses of other approaches. The Digibotics and Imageware systems are the only hardware/software combinations that provide automated digitizing and surfacing of complete complex objects. This capability to recreate 3D objects with this process is available now for applications such as creating spare parts, recreating parts where no prints or CAD model exist, and creating a CAD model from a physical model done in clay, foam, or other fragile material.